Bunching of cars in asymmetric exclusion models for freeway traffic

Takashi Nagatani
College of Engineering, Shizuoka University, Hamamatsu 432, Japan
(Received 2 May 1994)

One-dimensional cellular automaton (CA) models are presented to simulate bunching of cars in freeway traffic. The CA models are three extended versions of the asymmetric simple-exclusion model with parallel dynamics. In model I, the inherent velocities of individual cars are taken into account. It is shown that bunching of cars occurs since the car with low velocity prevents the car with high velocity from going ahead. The mean interval $\langle \Delta x \rangle$ of consecutive cars scales as $\langle \Delta x \rangle \approx t^{0.47\pm0.03}$ where t is time. In model II, the asymmetric exclusion model is extended to take into account the dependence of the transition probability T upon the interval Δx of consecutive particles (cars): $T=\Delta x^{-\alpha}$ $(\alpha \geq 0)$. It is shown that the mean interval $\langle \Delta x \rangle$ of consecutive particles scales as $\langle \Delta x \rangle \approx t^{1/(1+\alpha)}$ by bunching of cars. In model III, the velocity v of a car depends on the interval Δx of consecutive cars in such a manner that the transition probability $T=1$ for $\Delta x > x_c$ $(x_c \geq 1)$, and for $\Delta x \leq x_c$, $T=(\Delta x/x_c)^{\alpha}$. It is shown that a transition from laminar traffic flow (uncongested traffic flow) to congested traffic flow occurs with increasing density p of cars.

PACS number(s): 05.40.+j, 02.50.−r, 89.40.+k, 81.10.Bk

I. INTRODUCTION

Recently, traffic problems have attracted considerable attention. Traffic simulations based on various hydrodynamic models have provided much insight [1,2]. However, the simulation of traffic flow is a formidable task since it involves many degrees of freedom. Cellular automaton (CA) models are being applied successfully to simulations of complex physical systems [3,4]. The one-dimensional (1D) asymmetric exclusion model can be formulated as traffic jam problems. The 1D exclusion model is one of the simplest examples of a driven system [5,6]. The model has been extensively studied for understanding systems of interacting particles [7,8]. The 1D exclusion model is used to study the microscopic structure of shocks [9,10] and is closely linked to growth processes [11,12]. The two-dimensional versions of the asymmetric exclusion model were investigated by Biham, Middleton, and Levine [13] and other researchers [14–17] for simulating traffic flow in two dimensions.

Very recently, Nagel and Schreckenberg [18] introduced a stochastic cellular automaton model to simulate freeway traffic. They showed that a transition from laminar traffic flow to start-stop waves occurs with increasing car density as is observed in real freeway traffic. In their model, each car has an integer velocity v with values between zero and $v_{\max}$. Each car is accelerated, slowing down, randomized, or advanced by following four consecutive steps. However, the dependence of the velocity of start-stop waves on $v_{\max}$ and the randomization parameter is unclear. In their model, bunching of cars does not appear except for a single start-stop wave. Schadschneider and Schreckenberg [19] derived the exact results for the asymmetric exclusion process. They showed that bunching of cars over a distance of two lattice sites occurs due to an effective antiferromagnetic interaction.

Musha and Higuchi [20] have shown that traffic flow in a highway shows a $1/f$ power spectrum by measuring directly the traffic flow in a real highway. They have observed that cars flowing in a highway cluster more and more when moving ahead. They have suggested that the traffic flow is described by the Burgers equation. The Burgers equation is derived from the 1D asymmetric simple-exclusion model by an appropriate coarse graining [21]. The 1D asymmetric exclusion model is a microscopic model of the Burgers equation. The velocity field of the Burgers one-dimensional model of turbulence at extremely large Reynolds numbers is expressed as a train of random triangular shock waves. It has been shown that the number of shock fronts decreases with time as $t^{-\alpha}$ $(0<\alpha<1)$ and consequently the mean interval increases as t^{α} [22,23]. However, bunching (or clustering) of cars (or particles) never occurs in the 1D asymmetric simple-exclusion model. Kandel and Weeks [24] studied the step bunching in the different context of crystal growth. The step bunching problem is similar to that of car bunching.

Very recently, some interesting models were proposed for the density waves in traffic flow from the point of view of hydrodynamic models [25,26]. Leibig [26] studied the pattern-formation characteristics of interacting kinematic waves. He showed that a train of small density waves develops naturally to a large density wave. This characteristic is similar to that known in the Burgers equation. The interacting kinematic waves were observed in granular flow [27].

In this paper, we present the three CA models of freeway traffic showing bunching of cars. We extend the 1D asymmetric simple-exclusion model with parallel dynamics to take into account the car velocity. In real traffic, individual cars move with the inherent velocity if a car interacts with other cars. Each car adapts its velocity to the circumstances of traffic flow when a car interacts with other cars. Each car moves with a velocity depending upon the interval of consecutive cars. The velocity of cars is included in the transition probability in the asymmetric exclusion model. In model I, we consider the bunching of cars by the difference of velocities of cars. A velocity fluctuation of individual cars is taken into account where car i has the inherent velocity v_i. A car moving with lower velocity prevents a car moving with higher velocity from going ahead. Cars flowing in a highway cluster more and more when moving ahead. The bunching of cars is induced only by taking into account the differences of velocity between individual cars. We study the scaling behavior of the mean interval of cars and the distribution of the interval of consecutive cars.

In models II and III, we consider the bunching of cars by the interaction of consecutive cars. The interaction depends on the interval between consecutive cars. In model II, the dependence of the car velocity upon the interval Δx of consecutive cars is taken into account. At each time, the velocity of individual cars is determined by the function of the interval Δx. We consider the case in which the transition probability T is proportional to $(\Delta x)^{-\alpha}$ $(\alpha \geq 0)$. This means that the car velocity is proportional to the power of the interval. We show that the mean interval $\langle \Delta x \rangle$ of consecutive cars scales as $\langle \Delta x \rangle \approx t^{\beta}$. The dependence of the scaling exponent β upon the exponent α is shown.

In model III, we consider the effect to the safety distance on the traffic flow. A car moves with the maximal velocity if the interval of the consecutive car is larger than the safety distance. When the interval is less than the safety distance, the car moves with a low velocity proportional to the interval. We introduce the critical distance x_c into the dependence of car velocity upon the interval. The critical distance corresponds to the safety distance. A car moves with velocity 1 if the interval Δx of consecutive cars is larger than the critical distance x_c. When $\Delta x \leq x_c$, the velocity v decreases with Δx in such a manner that $v \approx (\Delta x / x_c)^{\alpha}$. The dynamical transition between the laminar traffic flow and the congested traffic flow occurs. In the congested traffic flow, start-stop waves appear and they interact with each other. We show the traffic current, the phase diagram, and the dependence of start-stop waves on the critical distance x_c.

The organization of the paper is as follows. In Sec. II we present model I for bunching of cars. We show the simulation result. In Sec. III we propose model II for car bunching. We study the scaling behavior of the interval of consecutive cars. In Sec. IV we present model III. We show the simulation result. Finally, Sec. V contains a discussion and a brief summary.

II. MODEL I AND SIMULATION

We consider cars flowing in a highway where each car has the inherent velocity. We try to simulate the traffic flow by as simple a model as possible. We extend the 1D asymmetric simple-exclusion model with parallel dynamics to take into account the inherent velocity of cars. The CA model is defined on a one-dimensional lattice of L sites with periodic boundary condition. Each site is occupied by a single car or it is empty. For an arbitrary configuration, one update of the system consists of the following rule which is performed in parallel for all cars. Car i moves ahead by one step with the inherent probability p_i, or otherwise, car i does not move with the probability $1-p_i$. In the dilute limit of car density, car i moves ahead with the mean velocity p_i at coarse-grained time scales since car i is not blocked by other cars. The probability p_i corresponds to the inherent velocity v_i of individual cars if car i is not blocked by other cars. When the probability $p_i = 1$ for all cars, model I reproduces the 1D asymmetric simple-exclusion model. Car i with lower probability p_i prevents car j with higher probability p_j $(p_j > p_i)$ from going ahead. Car j moves together with car i with an interval of a few sites. They form a cluster of cars. Furthermore, the cluster prevents car k with higher probability p_k $(p_k > p_i)$ from going ahead, or the cluster is prevented by car m with lower probability p_m $(p_m < p_i)$ from going ahead. The cluster grows more and more with moving ahead. Thus bunching of cars occurs without a specific attractive force. The bunching is due to the difference of velocity (transition probability p_i) between consecutive cars.

In this model, the traffic problem in a highway is reduced to its simplest form while the essential features are maintained. The feature includes the flow in one direction of cars which cannot overlap. Furthermore, this model possesses the property that the car moving with lower velocity prevents the car moving with higher velocity from going ahead.

We consider the simulation process of model I. Initially, cars are randomly distributed on the sites of one-dimensional lattice with car density p. Furthermore, the transition probability p_i is assigned to each car. The transition probability p_i assigned to each car does not change with time. We assume that the probability p_i is uniformly distributed between a and b. We set $a = 0.5$ and $b = 1.0$. The scaling behavior of the interval of consecutive cars depends little on the values a and b. Then, on each time step, if car i is not blocked ahead by another car, car i moves ahead with probability p_i, or otherwise, it does not move with probability $1-p_i$. If car i is blocked ahead by another car, car i does not move. One update of the system is performed in parallel for all cars.

We perform simulations of model I starting with an ensemble of random initial conditions where the system size is $L = 10^5$ and the initial density of cars is $p = 0.0-0.4$. Each run is calculated until 10^5 time steps. A clustering of cars occurs more and more with increasing time. We study the scaling behavior of the mean interval $\langle \Delta x \rangle$ between the car and the next car ahead. We define the mean interval $\langle \Delta x \rangle$ of consecutive cars as

$$\langle \Delta x \rangle \equiv \frac{\sum_{\Delta x=1}^{\infty} (\Delta x)^2 n_{\Delta x}}{\sum_{\Delta x=1}^{\infty} \Delta x n_{\Delta x}} , \tag{1}$$

where $n_{\Delta x}$ is the distribution of the interval Δx. Figure 1 shows the log-log plot of the mean interval $\langle \Delta x \rangle$ against

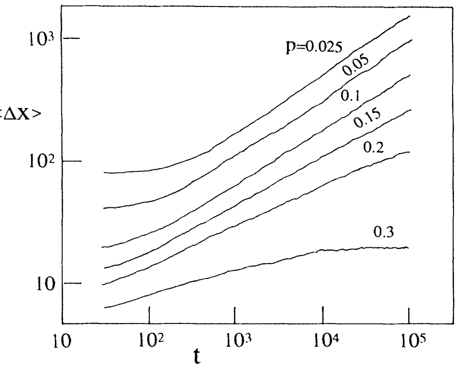

FIG. 1. The log-log plot of the mean interval $\langle \Delta x \rangle$ of consecutive cars against time t for densities $p=0.025$, 0.05, 0.1, 0.15, 0.2, and 0.3.

time t for the car densities $p=0.025$, 0.05, 0.1, 0.15, 0.2, and 0.3. For lower density than $p=0.1$, the mean interval $\langle \Delta x \rangle$ scales as

$$\langle \Delta x \rangle \approx t^{0.47\pm0.03} . \tag{2}$$

For $p>0.1$, the scaling (2) breaks down. For higher density than 0.3, the interval $\langle \Delta x \rangle$ approaches a constant value. In the dilute limit of car density p, the scaling exponent is consistent with the analytical result 0.5 derived from the Burgers equation [22,23] with numerical accuracy. Figure 2 shows the semilogarithmic plot of the cumulative interval distribution $N_{\Delta x}$ against the interval Δx for $t=10^3$, 5×10^3, 10^4, and 5×10^4 where $p=0.05$. The cumulative interval distribution $N_{\Delta x}$ is defined as $N_{\Delta x}=\sum_{\Delta x'=\Delta x}^{\infty} n_{\Delta x'}$. For many time steps, the cumulative interval distribution $N_{\Delta x}$ becomes nearly the exponential function. Figure 3 shows the semilogarithmic plot of the rescaled cumulative distribution $t^{0.47}N_{\Delta x}$ against the rescaled interval $t^{-0.47}\Delta x$ for $p=0.05$. The data collapse on a curve. We find that the cumulative interval distribution $N_{\Delta x}$ is described in terms of

$$N_{\Delta x} \approx \langle \Delta x \rangle^{-1} \exp\{-B\Delta x / \langle \Delta x \rangle\} , \tag{3}$$

where $\langle \Delta x \rangle \approx t^{0.47}$ and $B=0.19\pm0.03$ for $p=0.05$. The scaling form of the cumulative interval distribution

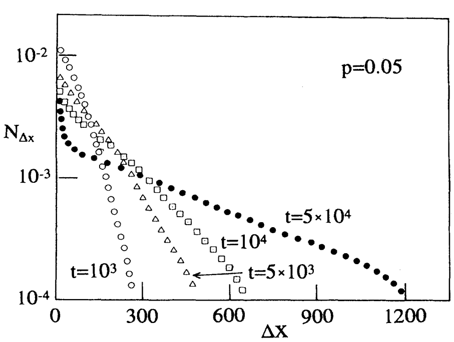

FIG. 2. The semilogarithmic plot of the cumulative interval distribution $N_{\Delta x}$ against the interval Δx for $t=10^3$, 5×10^3, 10^4, and 5×10^4 where $p=0.05$.

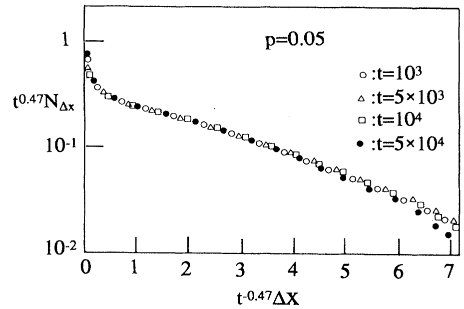

FIG. 3. The semilogarithmic plot of the rescaled cumulative interval distribution $t^{0.47}N_{\Delta x}$ against the rescaled interval $t^{-0.47}\Delta x$ for the data in Fig. 2.

agrees with the analytical result derived from the Burgers equation [22,23].

We study the scaling behavior of the mean cluster size $\langle s \rangle$ of cars. A cluster of cars is defined as a group of cars of which the interval is within the distance x_c. The cluster size of cars depends on the distance x_c. However, the scaling behavior is not very dependent upon the distance x_c. The mean cluster size $\langle s \rangle$ of cars is defined the same as Eq. (1). For lower density than $p=0.1$, the mean cluster size scales as Eq. (2) with the same scaling exponent. The scaling exponent of the mean cluster size agrees with the exponent of the mean interval. The semilogarithmic plot of the rescaled cumulative distribution $t^{0.47}N_s$ against the rescaled cluster size $t^{-0.47}s$ collapses nearly on a curve for $p=0.025$. We find that the cumulative cluster size distribution N_s is described in terms of

$$N_s \approx \langle s \rangle^{-1} \exp\{-Cs/\langle s \rangle\} , \tag{4}$$

where $\langle s \rangle \approx t^{0.47}$ and $C=5.43\pm0.03$ for $p=0.025$. The scaling form of the cumulative cluster size distribution is consistent with that of the cumulative interval distribution except for the constants B and C.

III. MODEL II AND SIMULATION

We present model II and study the scaling behavior of the mean interval $\langle \Delta x \rangle$ for car bunching. In model II, the dependence of velocity upon the interval Δx is taken into account. The dependence of velocity is introduced into the transition probability T of particles. We extend the 1D asymmetric simple-exclusion model with parallel dynamics to take into account the dependence of the transition probability T of particle (or car) upon the interval of consecutive particles. The transition probability T depends only on the distance Δx between the car and the next car ahead. It is given by

$$T=\Delta x^{-\alpha} . \tag{5}$$

The transition probability T decreases with increasing interval Δx. The transition probability changes with time since it depends on the interval of the consecutive car. For an arbitrary configuration, one update of the system consists of the following rule, which is performed in parallel for all cars. When a car is blocked ahead by another car, it does not move ahead. If a car is not blocked by another car, it moves ahead by one step with probability $\Delta x^{-\alpha}$ ($\alpha \geq 0$), or otherwise, it does not move with probability $1-\Delta x^{-\alpha}$. In the case of $\alpha > 0$, a clustering or bunching of cars occurs. Cars with shorter interval cluster more and more with moving ahead. Bunching of cars occurs with increasing time.

We study the scaling behavior of the mean interval $\langle \Delta x \rangle$ of consecutive cars. The mean interval is defined by Eq. (1). We perform simulations starting with an ensemble of random initial conditions where the system size is $L=10^5$, the initial density of cars is $p=0.0-0.5$, and the power α is $\alpha=0.05-2.0$. Each run is calculated until 10^5 time steps. At each time step, the transition probability of individual particles is calculated by Eq. (5). All particles are updated in parallel with the transition probability calculated at each time step. Figure 4 shows the log-log plot of the mean interval $\langle \Delta x \rangle$ against time t for car densities $p=0.05$, 0.1, 0.2, and 0.3 where $\alpha=0.2$. For low density $p=0.3$, the mean interval scales as

$$\langle \Delta x \rangle \approx t^{\beta}\ , \quad \text{with } \beta=0.81\pm0.02\ . \tag{6}$$

For lower density than $p=0.3$, the mean interval crosses over the straight line (6) with increasing time. The mean interval $\langle \Delta x \rangle$ is a characteristic length in the car bunching. The characteristic length diverges as the power law (6). We study the dependence of the scaling exponent β of the mean interval upon the power α. Figure 5 shows the log-log plot of the mean interval $\langle \Delta x \rangle$ against time t for the powers $\alpha=0.3$, 0.5, 0.7, and 0.9 where the car density $p=0.2$. The scaling exponent β of the mean interval decreases with increasing power α. Figure 6 shows the plot of the scaling exponent β against α. The curve represents the relation

$$\beta=1/(1+\alpha)\ . \tag{7}$$

The data agree with relation (7). The scaling relation (7) is derived from a simple scaling argument as follows. The increment $\Delta(\Delta x)$ of the typical interval Δx is proportional to the transition rate $(\Delta x)^{-\alpha}\Delta t$ that cars move ahead within the time period Δt:

$$d\Delta x/dt \approx \Delta x^{-\alpha}\ . \tag{8}$$

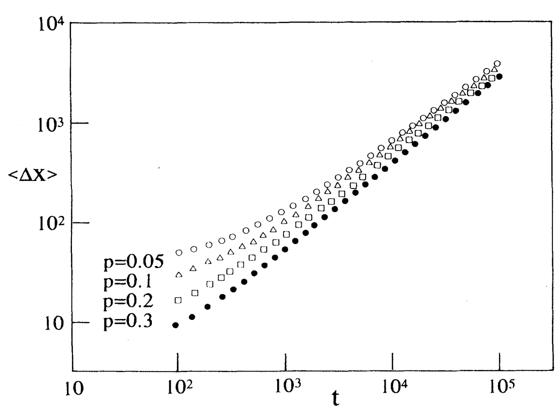

FIG. 4. The log-log plot of the mean interval $\langle \Delta x \rangle$ against time t for densities $p=0.05$, 0.1, 0.2, and 0.3 where $\alpha=0.2$.

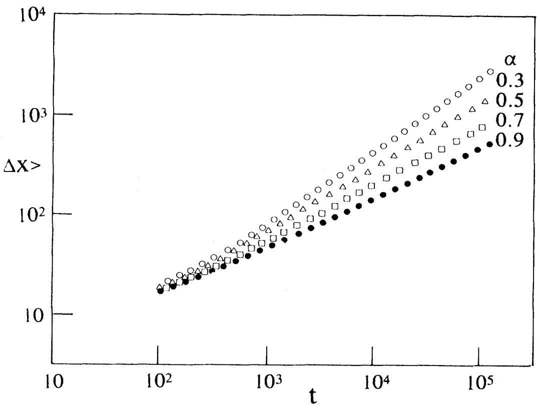

FIG. 5. The log-log plot of the mean interval $\langle \Delta x \rangle$ against time t for power $\alpha=0.3$, 0.5, 0.7, and 0.9 at density $p=0.2$.

The typical interval Δx scales as $\Delta x \approx t^{1/(1+\alpha)}$. Relation (7) is obtained.

We study the cumulative distribution $N_{\Delta x}$ of the interval Δx. Figure 7 shows the semilogarithmic plot of the cumulative interval distribution $N_{\Delta x}$ against interval Δx for $t=10^3$, 5×10^3, 10^4, and 2×10^4 where $p=0.2$ and $\alpha=0.5$. In order to investigate the scaling form of the cumulative interval distribution, we plot the rescaled cumulative distribution against the rescaled interval. Figure 8 shows the semilogarithmic plot of the rescaled cumulative distribution $t^{0.645}N_{\Delta x}$ against the rescaled interval $t^{-0.645}\Delta x$ for the data in Fig. 7. The data collapse on a curve. We find that the cumulative interval distribution is described in terms of

$$N_{\Delta x} \approx \langle \Delta x \rangle^{-1} f(\Delta x/\langle \Delta x \rangle)\ , \tag{9}$$

where $\langle \Delta x \rangle \approx t^{\beta}$ and the scaling function $f(x)$ is nearly a Gaussian distribution.

In model II, the car bunching (or clustering) occurs since the transition probability (or velocity) of cars increases with decreasing interval of consecutive cars.

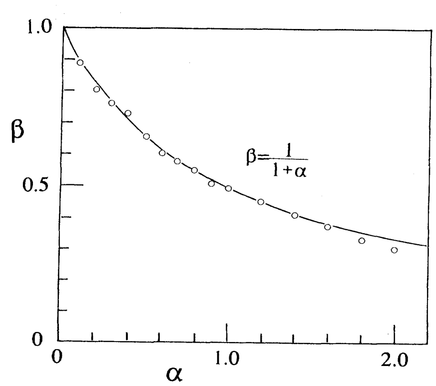

FIG. 6. The plot of the scaling exponent β against the power α.

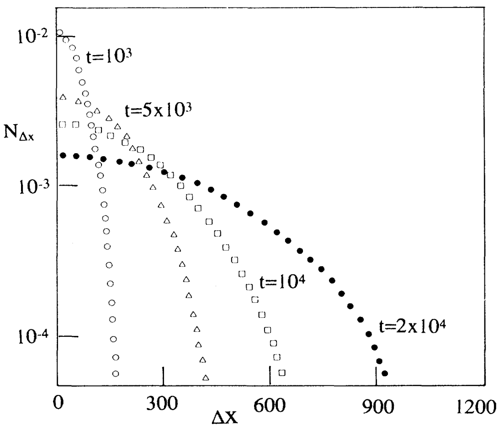

FIG. 7. The semilogarithmic plot of the cumulative interval distribution $N_{\Delta x}$ against the interval Δx for $t=10^3$, 5×10^3, 10^4, and 2×10^4 where $p=0.2$ and $\alpha=0.5$.

IV. MODEL III AND SIMULATION

We present model III. We study the effect of the safety distance on the traffic flow. We show the dynamical transition between the laminar traffic flow and the congested traffic flow. The critical distance x_c is introduced into the dependence of car velocity upon the interval. The critical distance corresponds to the safety distance. When the interval between consecutive cars is larger than the safety distance, the car moves with the maximal velocity. If the interval is less than the safety distance, the car moves with low velocity. We extend the 1D asymmetric exclusion model as follows. When the distance Δx between a car and the next car ahead is larger than the critical distance x_c and the car is not blocked ahead by another car, the car moves ahead by one step. If the interval Δx is equal to the critical distance x_c or smaller than x_c, and the car is not blocked ahead by another car, the car moves ahead by one step with probability $(\Delta x/x_c)^\alpha$ $(\alpha>0)$, or otherwise does not move ahead with probability $1-(\Delta x/x_c)^\alpha$. When the car is blocked ahead by another car, it does not move even if the blocking car moves out of the site during the same time step. For an arbitrary configuration, one update of the system is performed in parallel for all cars. Then, the transition probability T is given by

$$T=1 \quad \text{for } \Delta x>x_c \text{ and } T=(\Delta x/x_c)^\alpha \quad \text{for } \Delta x\le x_c\ . \tag{10}$$

The parameter α represents the dependence of car velocity v on the interval Δx of consecutive cars. In the limit of $x_c=1$, model III reproduces the 1D asymmetric simple-exclusion model.

We perform simulations of model III starting with an ensemble of random initial conditions where the system size is $L=10^4$, the initial density of cars is $p=0.0-1.0$, and the critical distance is $x_c=1-10$. Each run is calculated until 10^4 time steps. The data are averaged over 50 runs. At $p=0.1$, the start-stop wave is formed at an initial stage but disappears in due course of time. Finally, the traffic flow reaches a steady state in which the distance between a car and the next car ahead becomes larger than the critical distance x_c and all cars move with maximal velocity $v=1$. For $p=0.3$, a typical start-stop wave is formed, propagates backward throughout the space, and they interact with each other. Figure 9 shows the plot of the velocity v_w of the start-stop wave against the critical distance x_c for $p=0.4$ and $\alpha=1.0$. The data points are indicated by the circles. The solid curves indicates the function $1/x_c$. The velocity of the start-stop wave is proportional to the inverse of the critical distance:

$$v_w\approx 1/x_c\ . \tag{11}$$

The velocity v_w depends strongly on the distance x_c. It depends little on the car density p and the parameter α.

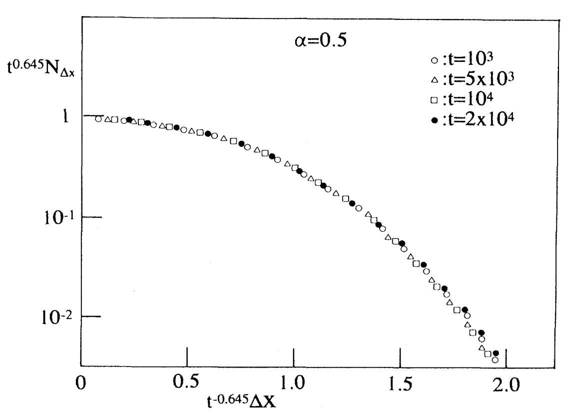

FIG. 8. The semilogarithmic plot of the rescaled cumulative distribution $t^{0.645}N_{\Delta x}$ against the rescaled interval $t^{-0.645}\Delta x$ for the data in Fig. 7.

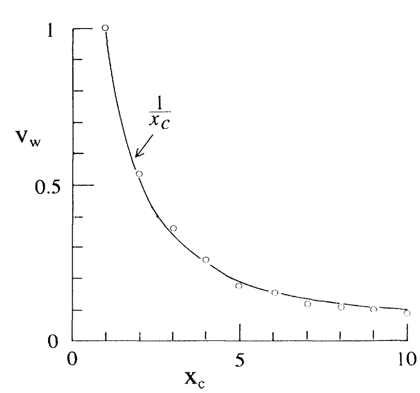

FIG. 9. The plot of the velocity v_w of the start-stop wave against the critical distance x_c for $p=0.4$ and $\alpha=1.0$. The solid curve indicates the function $1/x_c$.

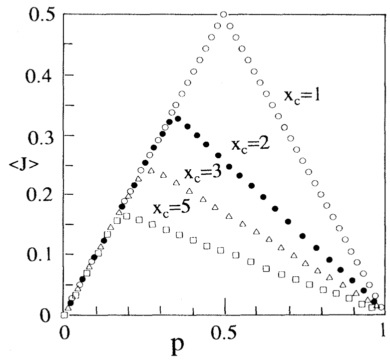

FIG. 10. The plot of the mean traffic current $\langle J \rangle$ against car density p for $x_c=1$ (white circles), 2 (black circles), 3 (triangles), and 5 (squares) where $\alpha=1.0$.

Figure 10 shows the plot of the mean traffic current $\langle J \rangle$ against car density p for the critical distance $x_c=1,2,3,5$ and $\alpha=1.0$. The mean traffic current $\langle J \rangle$ is obtained by averaging over 3000 times steps except the initial stage. The current $\langle J \rangle$ for $x_c=1$ represents that of the 1D asymmetric simple-exclusion model. The profile of current changes significantly with the critical distance x_c. For low values of car density p, the current agrees with that of the 1D asymmetric exclusion model. In the values of car density, all cars move ahead with the maximal velocity $v=1$. For high values of car density, the current becomes less with the critical distance x_c. Figure 11 shows the phase diagram between the car density p and the critical distance x_c for $\alpha=1.0$. The data points are indicated by the circles. The data are on the curve $1/(x_c+1)$. The region on the left-hand side of the curve represents the laminar traffic flow (uncongested traffic flow). The region on the right-hand side of the curve represents the congested traffic flow in which start-stop waves are formed and interact with each other. The dynamical transition point p_c between the laminar flow and the congested traffic flow is given by

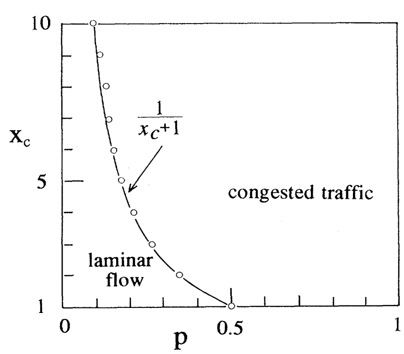

FIG. 11. The phase diagram between car density p and critical distance x_c for $\alpha=1.0$. The solid curve indicates the function $1/(x_c+1)$. The region on the left-hand side of the curve represents the laminar traffic flow. The region on the right-hand side of the curve represents the congested traffic flow in which start-stop waves are formed and interact with each other.

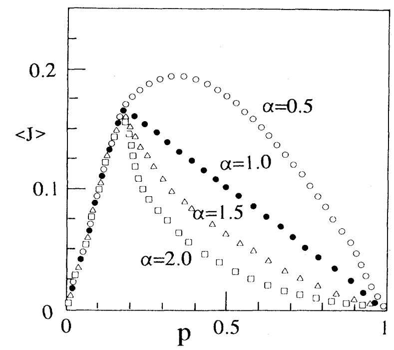

FIG. 12. The plot of the traffic current $\langle J \rangle$ against car density p at $x_c=5$ and $\alpha=0.5$ (white circles), 1.0 (black circles), 1.5 (triangles), and 2.0 (squares).

$$p_c \approx 1/(x_c+1) \; . \tag{12}$$

Figure 12 shows the plot of traffic current $\langle J \rangle$ against car density p at the critical distance $x_c=5$ for various values of the power α. The current profile depends on the power α. However, the transition point p_c changes little with the power α. The traffic current $\langle J \rangle$ agrees with that (represented by the straight line) of the 1D asymmetric exclusion model until the transition point p_c. For the regions of the congested traffic flow, the current decreases with increasing power α. For $\alpha>1$, the maximum value of current depends little on the power α. For $0<\alpha<1$, the maximum value of current increases with decreasing α.

V. DISCUSSION AND SUMMARY

We compare models I, II, and III with other models. In models I and II, car bunching occurs without stopping cars. All cars are always moving ahead. However, in Nagel and Schreckenberg's CA model, car bunching appears as a start-stop wave. Cars are always stopped. In Kerner and Kohnhauser's continuum model, car bunching occurs as a density wave and it propagates backward. Cars are always stopped. In Burgers turbulence, a train of shocks coalesces with forward propagation. The bunching behavior of models I and II is similar to that of Burgers turbulence. On the other hand, in model III car bunching appears as start-stop waves. The behavior is similar to that of Nagel and Schreckenberg's model.

In summary, we presented the three CA models for car bunching in a highway. In model I, we introduced the inherent transition probability of each particle into the 1D asymmetric exclusion model to take into account the inherent velocity of each car. We showed that car bunching occurs due to the difference of the inherent velocity and the mean interval $\langle \Delta x \rangle$ of consecutive cars scales as $\langle \Delta x \rangle \approx t^{0.5}$. In model II, we took into account the dependence of car velocity upon the interval of consecutive cars. We found that the mean interval of consecutive cars scales as $\langle \Delta x \rangle \approx t^{1/(1+\alpha)}$ by car bunching where the transition probability $T=\Delta x^{-\alpha}$. In model III, the critical distance x_c was introduced for the safe interval of consecutive cars. We showed that the transition occurs from laminar traffic flow to congested traffic flow.

ACKNOWLEDGMENT

We would like to thank Professor H. E. Stanley for helpful discussions.

[1] *Transportation and Traffic Theory,* edited by N. H. Gatner and N. H. M. Wilson (Elsevier, New York, 1987).
[2] W. Leutzbach, *Introduction to the Theory of Traffic Flow* (Springer, Berlin, 1988).
[3] S. Wolfram, *Theory and Applications of Cellular Automata* (World Scientific, Singapore, 1986).
[4] K. Kaneko, in *Formation, Dynamics and Statistics of Patterns,* edited by K. Kawaskai, M. Suzuki, and A. Onuki (World Scientific, Singapore, 1990), Vol. 1, p. 1.
[5] T. M. Liggett, *Interacting Particle Systems* (Springer, New York, 1985).
[6] H. Spohn, *Large Scale Dynamics of Interacting Particles* (Springer, Berlin, 1991).
[7] B. Derrida, M. R. Evans, V. Hakim, and V. Pasquier, J. Phys. A **26**, 1493 (1993).
[8] L. H. Gwa and H. Spohn, Phys. Rev. Lett. **68**, 725 (1992).
[9] S. A. Janowsky and J. L. Lebowitz, Phys. Rev. A **45**, 618 (1992).
[10] M. Bramson, J. Stat. Phys. **51**, 863 (1988).
[11] P. Meakin, P. Ramanlal, L. M. Sander, and R. C. Ball, Phys. Rev. A **34**, 5091 (1986).
[12] J. Krug and H. Spohn, Phys. Rev. A **38**, 4271 (1988).
[13] O. Biham, A. A. Middleton, and D. Levine, Phys. Rev. A **46**, 6124 (1992).
[14] T. Nagatani, J. Phys. Soc. Jpn. **62**, 2625 (1993).
[15] M. Fukui and Y. Ishibashi, J. Phys. Soc. Jpn. **62**, 3841 (1993).
[16] T. Nagatani, Phys. Rev. E **48**, 3290 (1993).
[17] J. A. Cuesta, F. C. Martinez, J. M. Molera, and A. Sanchez, Phys. Rev. E **48**, 4175 (1993).
[18] K. Nagel and M. Schreckenberg, J. Phys. (France) I **2**, 2221 (1992).
[19] A. Schadschneider and M. Schreckenberg, J. Phys. A **26**, L679 (1993).
[20] T. Musha and H. Higuchi, Jpn. J. Appl. Phys. **17**, 811 (1978).
[21] J. L. Lebowitz, E. Presutti, and H. Spohn, J. Stat. Phys. **51**, 841 (1988).
[22] T. Tatsumi and S. Kida, J. Fluid Mech. **55**, 659 (1972).
[23] S. Kida, J. Fluid Mech. **93**, 337 (1979).
[24] D. Kandel and J. Weeks, Phys. Rev. Lett. **69**, 3758 (1992).
[25] B. S. Kerner and P. Kohnhauser, Phys. Rev. E **48**, 2335 (1993).
[26] M. Leibig, Phys. Rev. E **49**, 184 (1994).
[27] J. Lee, Phys. Rev. E **49**, 281 (1994).